Water Resources Research

RESEARCH ARTICLE
10.1029/2020WR028286

Special Section:
Advancing process representation in hydrologic models: Integrating new concepts, knowledge, and data

Key Points:
- Evaporation with dry soil layer (DSL) investigated with laboratory experiments using soil columns under different evaporation conditions
- Atmospheric pressure fluctuation has a large effect on the evaporation with thick DSL
- Both daily changes in solar radiation and different DSL thickness had only a limited effect on soil evaporation with a thick DSL

Supporting Information:
Supporting Information may be found in the online version of this article.

Correspondence to:
E. Balugani,
e.balugani@utwente.nl;
enrico.balugani2@unibo.it

Citation:
Balugani, E., Lubczynski, M. W., & Metselaar, K. (2021). Evaporation through a dry soil layer: Column experiments. *Water Resources Research*, *57*, e2020WR028286. https://doi.org/10.1029/2020WR028286

Received 2 JUL 2020
Accepted 23 APR 2021

Evaporation Through a Dry Soil Layer: Column Experiments

E. Balugani[1], M. W. Lubczynski[1], and K. Metselaar[2]

[1]University of Twente, Faculty of Geoinformation Science and Earth Observation ITC, Enschede, The Netherlands,
[2]Wageningen University, Wageningen, The Netherlands

Abstract Modeling of water vapor transport through a dry soil layer (DSL), typically formed in the top soil during dry seasons in arid and semi-arid areas, is still problematic. Previous laboratory experiments in controlled environments showed that the only vapor transport process through the DSL is by Fick's law of diffusion. However, field experiments exhibited consistently higher evaporation rates than predicted by diffusion flow only. Some proposed reasons for the mismatch were: (a) daily cycles of condensation and evaporation in the DSL due to changes in solar radiation; (b) wind effects on air movement in the DSL; (c) atmospheric pressure fluctuations; (d) nonlinear influence of the DSL thickness on the evaporation process. To link the laboratory experiments with field observations, we performed soil column experiments in the laboratory with thick (>50 cm) DSL, and with different wind speeds, two radiative lamp schedules (continuous and 12 h daily cycles) and different thicknesses of DSL. Atmospheric pressure, air temperature and humidity were measured continuously. The results show that the evaporation rates observed are larger than those predicted by diffusion flow only. We found that it was possible to model the evaporation rates as a function of atmospheric pressure fluctuations. In conclusion, atmospheric pressure fluctuations can induce evaporation rates in DSL larger than estimated by diffusion flow only, possibly explaining the discrepancy between laboratory and field evaporation rates.

1. Introduction

Evaporation is one of the main components of the hydrologic cycle in semi-arid and arid areas, where topsoil (the first few decimeters of soil material) is often very dry, especially during dry season (Wang, 2015). Such areas, often referred to as water limited environments (Parsons & Abrahams, 1994) are characterized by low precipitation and high potential evaporation rates; the precipitation events are mostly concentrated in few months (wet season) but rare during the rest of a year, when long periods of droughts are common (dry season).

When a dry spell is long enough for evaporation to deplete the soil moisture in a topsoil, a dry soil layer (DSL) forms, that is, a layer where water moves only in vapor form (Brutsaert, 2014; Or et al., 2013). Semi-arid and arid regions are generally characterized by sandy soils (Bestelmeyer et al., 2015); hence, most of the time, a thick (5–50 cm) DSL is present in the topsoil (Koonce, 2016; Wang, 2015). During the dry season, due to the high potential evaporation, the top soil becomes increasingly dry and the short precipitation events typically infiltrate only the first few centimeters of soil and quickly evaporate (Sun et al., 2016).

The evaporation process from an initially saturated soil material is thought to occur in two stages (Or et al., 2013): during the first stage the depth of the upper boundary of the saturated zone (the drying front, equivalent to the upper boundary of the capillary rise from the saturate zone, Figure 1) increases because of the loss of water through upward transport in the liquid phase to the ground surface, where evaporation takes place. When the drying front reaches a certain depth, liquid water continuity with the surface is disrupted and a DSL is formed between the ground surface and the vaporization plane, that is, the plane from which all the water moves by vapor to the surface, with depth determined by soil material properties and soil temperature (Figure 1, Lehmann et al., 2008; Neriah et al., 2014). This is the beginning of the second stage of evaporation, when there is a zone through which liquid water moves upward from the drying front to the vaporization plane (Figure 1) where it evaporates and is transported as water vapor through the DSL to the surface (Shokri et al., 2009).

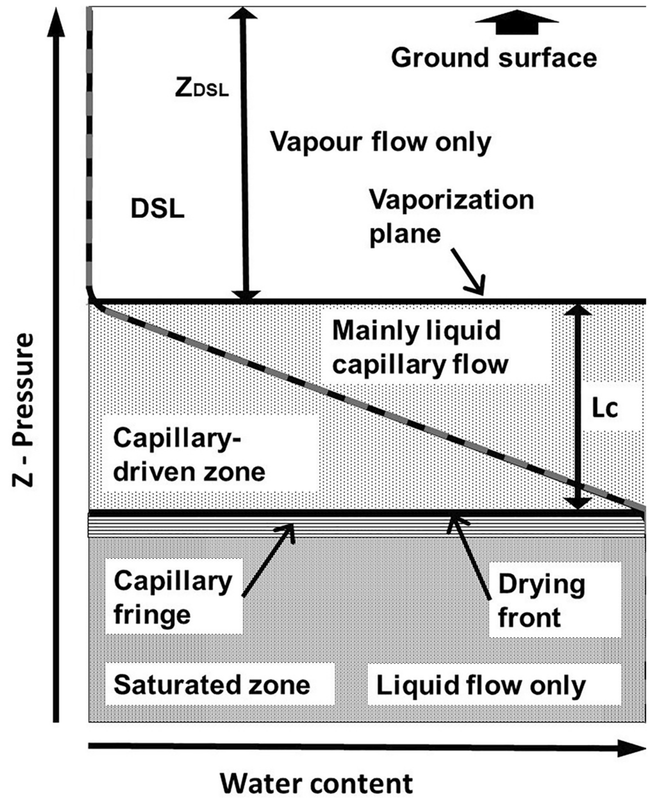

Figure 1. Water content in a soil material during the second stage of evaporation (modified after Shokri & Salvucci, 2011). The soil material profile is divided into three zones: (a) saturated zone, overlain by the capillary fringe, bounded at the top by a drying front; (b) unsaturated zone, where water moves upward by capillary flow from the drying front to the vaporization plane; (c) a dry soil layer (DSL) where water moves only as water vapor. The black curve is an example of the soil water saturation profile and the superimposed dashed gray line is the linearization of the retention curve.

The development of an air-dry DSL has been observed in laboratory experiments (e.g., Or et al., 2013). Most of such experiments were performed on initially saturated sandy soil columns of a few decimeters height under controlled, stable evaporative conditions and at a bottom boundary conditions of either no-flow (Lehmann et al., 2008), or a fixed matric potential head (Shokri & Salvucci, 2011). Or et al. (2013) review of laboratory studies summarized the following observations: (a) evaporation rates during the second stage were independent from the rates of the first stage, (b) the evaporation did not change much (remaining as lower than 1 mm d^{-1}) over a wide range of boundary conditions and soil textures, and (c) the observed evaporation rates can be described using Fick's law of diffusion (from here on referred to simply as diffusion).

The development of a DSL has also been observed in field studies (Assouline et al., 2013; Deol et al., 2014; Dijkema et al., 2017; Sun et al., 2016); however, in contrast to laboratory column experiments, the evaporation rates observed in the field were higher than the rates predicted using only diffusion flow. Besides, there seems to be no agreement yet on the process(es) involved in the transport of water through the DSL, which would explain the different results in field and laboratory conditions. The development of a DSL has been observed in the field in different climates during long drying spells. The DSL thickness (Z_{DSL}) varied from a few millimeters in a humid sub-tropic climate (Deol et al., 2014), to more than 50 cm in a desert climate (Sun et al., 2016). In field conditions, a DSL is usually observed using destructive sampling of the topsoil (Assouline et al., 2013) or through matric potential measurements (Dijkema et al., 2017).

In most field studies where the reported Z_{DSL} was only a few centimeters thick, it was possible to simulate the observed evaporation rates using models that ignored the liquid water discontinuity, that is, ignoring the DSL, or even ignoring vapor flow altogether (Assouline et al., 2013; Brutsaert, 2014). The fact that a DSL of a few centimeters thick had a negligible effect on the evaporation rates was explained by proposing a number of possible processes that enhance water vapor transport through the DSL; processes such as the condensation and evaporation of water vapor in the DSL due to solar-driven daily cycles and the effect of air turbulence on the first centimeters of soil, are often not reproduced in laboratory conditions (Brutsaert, 2014). However, Shokri and Or (2011) showed that, when applying only liquid flow during model simulations, agreement between observed and simulated evaporation rates might have been obtained by adjustments of the (unknown) fitting parameters of the unsaturated hydraulic conductivity function, potentially misrepresenting the actual transport process.

Direct field observations showed daily changes of Z_{DSL} in the order of few centimeters, attributed to condensation at the bottom of the DSL and evaporation at the vaporization plane (Assouline et al., 2013). Assouline et al. (2013) suggested that these daily changes increase the water vapor diffusion through the DSL by: (a) decreasing the diffusion path length, and (b) storing a certain amount of liquid water close to the soil surface, available for evaporation in the early morning (Brutsaert, 2014; Idso et al., 1979). This results in evaporation rates comparable to those calculated for continuous liquid water upward flow through the soil, as discussed in Assouline et al. (2013) and Brutsaert (2014).

Another mechanism for water vapor transport through a DSL is air advection, which can be induced in the soil material by changes of air pressure at the surface, due to wind or barometric pressure variations. Davarzani et al. (2014) conducted soil column evaporation experiments in a wind tunnel that showed that warm, dry wind with fluctuating speeds has no effect on second stage evaporation. Periodic changes in barometric pressure result in air being pumped in and out of the soil, a process called barometric pumping

(Kuang et al., 2013). The barometric pumping effect results in two modes of transport in the gas phase: direct advection up and down due to changes in gas phase pressure, and mechanical dispersion resulting from such pumping, as described in Auer et al. (1996). Grifoll (2013) used a numerical model to study the effects of three causes of mechanical dispersion on evaporation through a DSL: (a) temperature variations which, since water vapor pressure is dependent on temperature, create a thermally induced flow (Zeng et al., 2009), (b) barometric pumping, that had a negligible effect, and (c) Stefan flow (Lampinen et al., 2001) that had magnitude similar to the flow due to vapor diffusion, although that the model refered to the specific condition of loamy soil and Z_{DSL} of ∼1 cm.

Soil evaporation studies conducted in semi-arid and arid conditions (Balugani et al., 2018; Dijkema et al., 2017; Wang, 2015) show a significant effect of the DSL on evaporation rates when Z_{DSL} is larger than ∼5 cm. Wang (2015) reviewed several evaporation studies conducted in dry sandy soils, and showed that the effect of the DSL as a limiting factor on evaporation rates increases: linearly for $Z_{DSL} < 5$ cm, and logarithmically for $Z_{DSL} > 5$ cm. McColl et al. (2017) showed that the characteristic timescale of soil drying depends on both soil material properties and aridity index (defined in McColl et al., 2017, as the ratio between mean daily net radiation and latent heat of vaporization). Dijkema et al. (2017) found that the underestimation of lysimeter evaporation rates by a numerical model based on Richard's equation is due to difficulties in modeling the flow in dry conditions at the topsoil ($Z_{DSL} \sim 25$ cm). Finally, Balugani et al. (2018) observed a significant effect of DSL on the evaporation rates measured in a semi-arid area during the dry season, with a $Z_{DSL} \sim 25$ cm. Hence, the thickness of the DSL is a factor that needs to be controlled to systematically check possible explanations for differences between laboratory and field observations.

The aim of this study was to investigate the processes of water vapor transport through a thick DSL, imposing controlled laboratory conditions as close as possible to those observed in the field in semi-arid areas. The specific objectives of this study were to test, in a sandy soil with a thick DSL:

1. The commonly used assumption that the water transport through a thick DSL is by diffusion only
2. The DSL effects on the evaporation rates due to:
   - Daily cycles in solar radiation (implying temperature and relative humidity changes as well)
   - Wind speed changes (air turbulence)
   - Atmospheric pressure changes and the related barometric pumping and air advection effects

2. Materials and Methods

2.1. Soil Columns Design

For the experiment, we used two PVC columns with different heights and diameters (Figure 2, from here on referred to as short and long columns, respectively) both equipped with soil moisture, matric potential, and temperature sensors (Decagon, USA, Figure 2). The sensors were connected to a Campbell CR1000 data logger (Campbell Scientific, USA) recording data every 5 min. The bottoms of the columns were covered with 5 cm of gravel (5 mm size) separated from the overlying soil material by a perforated aluminum plate (with 3 mm holes). The columns were wrapped in glass wool to insulate their walls and to slow down lateral heat loss. A valve connected each column (1 cm above the bottom) to a Mariotte bottle in order to maintain a fixed water table depth (WTD) inside the columns. The Mariotte bottles were continuously weighed with digital balances (0.01 g accuracy). Since the water in the columns was in equilibrium with the water in the Mariotte bottles, and the only possible output of water from the Mariotte bottle-column system was as water vapor from the column top, then the change in weight of the Mariotte bottle represented water evaporation from the column.

The columns were filled with quartz sand sieved to select 0.1–0.25 mm particle size. After sieving, the sand was washed and oven dried. The sand was packed in the columns 1 cm at a time until the columns were completely filled. The final porosity of the sand was 0.40 (material density of ∼1.06 g cm^{-3}). The water retention curve for the sand material was determined using a Decagon WP4 dew point potentiometer (Decagon Devices, Pullman, WA, USA). The Z_{DSL} was calculated as $Z_{DSL} = \text{WTD} - L_c$, where L_c is the thickness of the capillary-driven zone (including the capillary fringe, Figure 1), which was determined from soil material properties alone as shown in Shokri and Salvucci (2011). In this study, the L_c for the material used

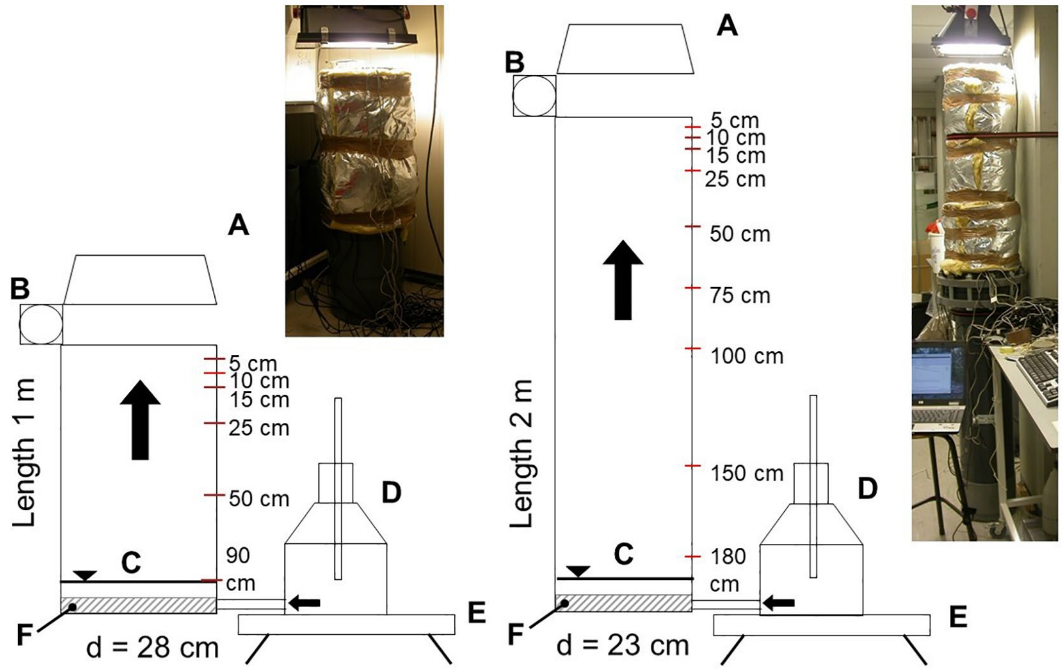

Figure 2. Geometry and experimental setup of the short and long columns: A—radiative lamp, B—fan, C—water table, D—Mariotte's bottle, E—digital balance, F—gravel layer (5 cm thick), and d—diameter of a column; the numbers at the right sides of the columns, represent depths of installation of the temperature and soil moisture/matric potential sensors.

was estimated to be 10 cm based on the grain size analysis and confirmed by direct observation through destructive sampling at the end of the experiment.

The top boundary conditions were set up using a radiative lamp (800 W maximum power), with a timer switch and a fan. The atmospheric pressure, continuously measured in the nearby (~1,500 m distance) weather station at the University, was representative for the atmospheric pressure inside the laboratory (not pressurized). The target evaporative conditions were typical for semi-arid conditions: maximum net radiation of 70 MJ m^{-2} d^{-1}; maximum top soil temperature ~75°C (with fan off); relative humidity of 20% at 10 cm above soil surface; evaporative conditions of 20 mm d^{-1}.

2.2. Diffusion Flow in a Thick DSL

To test the hypothesis that the only transport mechanism of water vapor through a thick DSL ($Z_{\mathrm{DSL}} > 50$ cm) is by diffusion (objective 1), we compared the observed evaporation rates from the columns with the corresponding theoretical rates of diffusion. This was done for different Z_{DSL}: if there was a proportionally inverse relationship between diffusion flow and Z_{DSL} (Equation 1), we would expect to see this relationship in the measured evaporation rates. The different evaporation rates were determined for three different water table heights (WTHs) above the column's bottom: 10, 20, and 30 cm corresponding to WTD of 90, 80, 70 cm in the short column and 190, 180, 170 cm in the long column.

Assuming that only water vapor diffusion takes place between the vaporization plane and the column surface (see Figure 1), the evaporation rate from a column filled with porous material can be calculated with Fick's law (Shokri et al., 2009) as:

$$E_{\mathrm{dif}} = D_{\mathrm{pm}}^{v} \frac{C_{\mathrm{sat}} - C_{\mathrm{air}}}{Z_{\mathrm{DSL}}} \quad (1)$$

Table 1
Sequence of Experimental Tests and Their Description

Test	Start	End	WTH [cm]	U [m s^{-1}]	Lamp schedule	Notes
T1	14 Oct 2011	18 Nov 2011	10	0	on 24 h	column's equilibration
T2	19 Nov 2011	04 Dec 2011	10	0	on 24 h	at equilibrium
T3	05 Dec 2011	11 Dec 2011	10	1.8	on 24 h	fan turned on
T4	12 Dec 2011	19 Dec 2011	20	1.8	on 24 h	WTH raised
T5	20 Dec 2011	22 Dec 2011	20	1.8	on 24 h	bottle test
T6	23 Dec 2011	12 Jan 2012	20	1.8	on/off 12 h	lamp 12 h cycle
T7	13 Jan 2012	08 Feb 2012	30	1.8	on/off 12 h	WTH raised
T8	09 Feb 2012	19 Feb 2012	30	0.3	on/off 12 h	slower wind speed

Note. WTH - water table height measured from the bottom of the column, U - wind speed. Every time the WTH was raised, the first 5 days of the Mariotte bottle weight datasets were considered as the equilibration period, so were not used in the evaporative rate calculations.

where c_{sat} and c_{air} are the vapor densities in soil pores at the vaporization plane (mol mol^{-1}) and in the air above the column surface respectively and D^{v}_{pm} (m^2 s^{-1}) is the diffusion coefficient for water vapor in the soil material, calculated as in Moldrup et al. (2000):

$$D^{v}_{pm} = \frac{S_g^{2.5}}{\phi} D_v^{air} \tag{2}$$

where S_g is the volumetric gas phase content in the soil material (equal to porosity in the DSL, both dimensionless), ϕ is the porosity and D_v^{air} is the diffusion coefficient of water vapor in free air (m^2 s^{-1}), corrected for the absolute mean temperature of the dry layer T (K) as $D_v^{air} = 0.22\left(T / 273\right)^{1.75}$.

2.3. Radiative Cycles and Stable Wind Effects on Vapor Transport Through a DSL

To test the effects on evaporation rates due to changes in radiation input and with different wind speed applied on the soil surface (addressing objectives 2a and 2b), and with different Z_{DSL}, we changed the experimental conditions and measured evaporation rates from the columns at equilibrium conditions. The experimental setup involved different Tests designated as T1 to T8 performed on both columns (Table 1), with WTH, wind speed (U), and radiative lamp schedule (LS) as Test factors. In every Test, only one variable was changed, and when the WTH was changed, the columns were left to equilibrate for ~14 days. We checked the statistical significance of the differences between evaporation rates measured in the Tests by using the ANOVA test to determine if groups of data were statistically different, and the Tukey post hoc test to assess which group of data differed from the others.

Therefore in: (T1) the water entered the columns while keeping them under constant evaporative conditions (fan turned off and radiative lamp turned on 24 h) until steady state was reached, with WTH = 10 cm (resulting in Z_{DSL} of 80 and 180 cm for the short and long column, respectively, due to L_c = 10 cm); (T2) the evaporation rates were measured after equilibrium was reached, with the same evaporative conditions as in the equilibrium period; (T3) the fan was turned on, creating a wind with speed = 1.8 m s^{-1}; (T4) the WTH was increased to 20 cm (resulting in Z_{DSL} of 70 and 170 cm for the short and long column, respectively); (T5) the connections between the Mariotte bottles and the columns were closed to test the experimental design for possible leakages; (T6) the radiative LS was changed to 12 h on/off cycles; (T7) the WTH was increased to 30 cm (resulting in Z_{DSL} of 60 and 160 cm for the short and long column, respectively); (T8) the fan power was decreased, resulting in a wind speed of 0.3 m s^{-1}.

2.4. Atmospheric Pressure Fluctuations Effects on Vapor Transport Through a DSL

2.4.1. Direct Barometric Pumping

To test the hypothesis that the water vapor transport through a thick DSL is a combination of diffusion and atmospheric pressure changes (objective 2c) as described by Auer et al. (1996), we compared the observed evaporation rates with the sum of the calculated diffusion and barometric pumping flow (advection). Changes in atmospheric pressure resulted in an up and down movement of the gas phase in the soil material with an amplitude that decreased with depth from the soil surface, resulting in a movement of water vapor (Massman, 2006). This gas phase movement resulted in: (a) a mix of the vapor in the gas phase near the surface with the air above the soil, shortening the distance traveled by water vapor by diffusion (the direct barometric pumping effect); (b) the mechanical dispersion of water vapor in the DSL, resulting in an increase of the diffusion coefficient proportional to the velocity of the gas phase (Grifoll, 2013).

Assuming that the atmospheric pressure fluctuations can be represented by a few low frequency Fourier components, each characterized by amplitude of pressure change ΔP (kPa), the deepest layer of gas phase mixed with air above the soil (i.e., affected by direct barometric pumping) is:

$$2\Delta L_{\text{pump}} \cong 2\frac{\Delta P}{P_0} Z_{\text{DSL}} \tag{3}$$

where P_0 is the average surface pressure (kPa) (for the full derivation of Equation 3, see Auer et al., 1996). Therefore, the actual distance traveled by water vapor by diffusion (L) is equal to the depth between the vaporization plane and the depth directly mixed by barometric pumping, that is, $L = Z_{\text{DSL}} - 2\Delta L_{\text{pump}}$.

2.4.2. Dispersion Due to Atmospheric Pressure Fluctuations

Another effect of atmospheric pressure fluctuations is the mechanical dispersion, which combined with water vapor diffusion ($E_{\text{dif+disp}}$ [mm d^{-1}]), can be expressed (Auer et al., 1996; Bear, 1972) as follows:

$$E_{\text{dif+disp}} = \left(D_{\text{pm}}^{v} + \alpha\left|V\right|\right)\frac{C_{\text{sat}} - C_{\text{air}}}{L} \tag{4}$$

$$V \cong -\frac{\Delta P}{P_0}\left(L - z\right)\omega\sin\left(\omega t\right) \tag{5}$$

where α is the dispersivity coefficient (m), $\left|V\right|$ is the positive measure of the pore scale velocity of the gas phase V (m s^{-1}), z is depth from the soil surface (m), and t is time (s). The term α depends on soil material properties at the scale of interest, so it depends on soil type, water vapor transport distance, and lateral scale of the experiment (Vanderborght & Vereecken, 2007). An estimate for α can be obtained from the data set of Vanderborght and Vereecken (2007), as in Grifoll (2013).

To test the effects of the mechanical dispersion due to atmospheric pressure changes, we checked the significance of the correlations between E and $\left|\Delta P\right|$ for all the tests boundary conditions. The combination of Equations 4 and 5 can be simplified as $E_{\text{disp}} = f\left(\left|V\right|\right)$ and $V \cong g\left(\Delta P\right)$. Combining the two equations results in $E_{\text{disp}} = f^\circ g\left(\Delta P\right) = h\left(\left|\Delta P\right|\right)$, with f and g some functions, and h a combination of them. Therefore, we can simplify the above approach by testing the hypothesis that there is significant correlation between changes in atmospheric pressure (ΔP [kPa d^{-1}]) and corresponding evaporation rates (E [mm d^{-1}]), i.e., $E = h\left(\left|\Delta P\right|\right)$. This can be done without any assumption regarding α values or distance traveled by water vapor. We also tested the correlations between the evaporation rates measured and the parameters characterizing the atmospheric pressure fluctuations, such as amplitude and frequency.

Simplifying Equation 4 by assuming constant diffusion flow and a constant vertical water vapor concentration gradient, we obtain the total evaporation rates as:

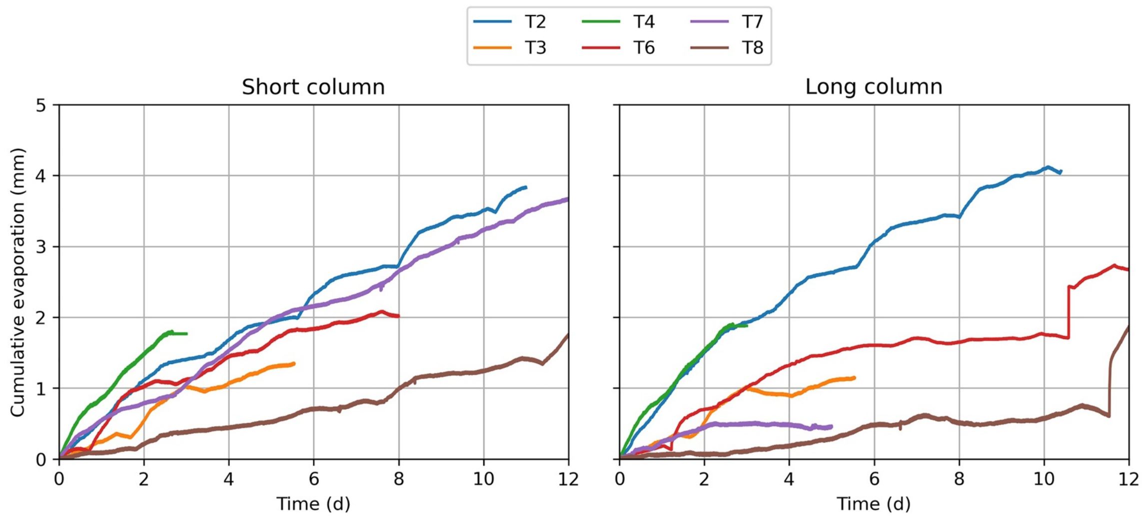

Figure 3. Cumulative evaporation (mm) for every experimental Test conducted in both columns.

$$E_{\mathrm{dif+disp}} = \left(D_{\mathrm{pm}}^{v} + \alpha\left|V\right|\right)\frac{dC}{dz} = D_{\mathrm{dif}}\frac{dC}{dz} + \alpha\left|V\right|\frac{dC}{dz} = \frac{dC}{dz}\alpha\left|-\frac{\Delta P}{P_0}\left(L - z\right)\omega\sin\left(\omega t\right)\right| + D_{\mathrm{pm}}^{v}\frac{dC}{dz} \tag{6}$$

Equation 6 can be simplified as:

$$E_{\mathrm{dif+disp}} \cong \left|-\Delta P \cdot k_1\right| + k_2 \tag{7}$$

$$\text{where: } k_1 = \frac{dC}{dz}\alpha\frac{1}{P_0}\left(L - z\right)\omega\sin\left(\omega t\right); k_2 = \left(D_{\mathrm{pm}}^{v}\frac{dC}{dz}\right).$$

where k_1, and k_2 are two constants used to fit the Equation 7, which suggests that evaporation rates should be correlated to the absolute value of the atmospheric pressure changes. To calibrate and validate the model we split the short column evaporation data set into two sets: calibration (T2, T3, and T4) and validation (T6, T7, and T9). The model was then used to simulate the long column evaporation to test its robustness by comparing the simulated with the measured data.

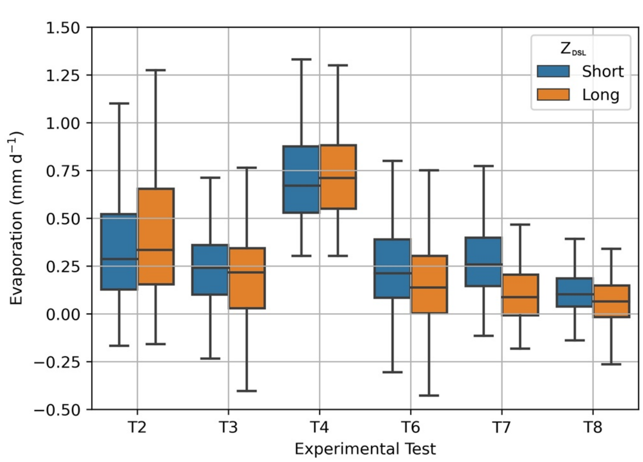

Figure 4. Boxplot of the evaporation rates for different experimental Tests for both short and long column.

3. Results

3.1. Soil Column Measurements

Figure 3 shows the cumulative evaporation of seven (T2–T7) experimental Tests at short and long columns; all the conducted Tests resulted in the continuous decrease of water from the Mariotte bottles, indicating outflow of water vapor (evaporation) from the columns. Since the soil was mostly dry, the rates of evaporation in all the Tests were relatively small (~0.3 mm d^{-1}) but varied among the Tests, as indicated by different slopes (discussed in Section 3.2) and by different, periodic fluctuations (discussed in Section 4.2) in the evaporation rates due to different evaporation conditions.

3.2. Statistical Analysis of Evaporation Rates With Different Evaporative Conditions

The measured evaporation rates from the two columns are shown in a boxplot in Figure 4. Some Tests, such as: T3 (changed wind speed), T6

Table 2

Comparison of Measured Average Daily Evaporation Rates With Evaporation Rates Calculated Using: (i) Diffusion Only (Equation 1); (ii) Diffusion With Barometric Pumping Effect Estimated as the Sum of Fick's Diffusion Flow and Direct Barometric Pumping Calculation (Substituting Equation 3 in Equation 1); (iii) Diffusion and Barometric Pressure Fluctuation Effect Estimated as the Sum of Diffusion Flow and the Effect of Barometric Pressure Fluctuation Calculated Using Equation 8, Calibrated Using the Short Column Dataset (Short-cal); Results are the Same for Both Columns

Evaporation (mm d^{-1})	Column	T2	T3	T4	T6	T7	T8
Measured	Short	0.350	0.240	0.728	0.277	0.286	0.127
	Long	0.408	0.207	0.755	0.241	0.118	0.066
Diffusion Only	Short	0.061	0.004	0.005	0.001	0.000	0.000
	Long	0.029	0.002	0.002	0.003	0.004	0.002
Diffusion with Barometric Pumping Effect	Short	0.077	0.008	0.008	0.004	0.002	0.005
	Long	0.043	0.011	0.011	0.009	0.009	0.010
Diffusion and Barometric Pressure Fluctuation Effect	Short-cal	0.265	0.328	0.344	0.344	0.256	0.226
Z_{DSL} (cm)	Short	80	80	70	70	60	60
	Long	180	180	170	170	160	160

Notes. All evaporations are in mm d^{-1}.

(increased WTH, changed LS), T7 (changed WTH), T8 (changed wind speed) show very similar evaporation rates (Figure 4). There is no clear difference in evaporation rates between the two columns with different Tests: in tests T3, T6, T7, and T8 the average evaporation rates seem to be slightly lower for the long column (with larger Z_{DSL}) than for the short column (with smaller Z_{DSL}) while in Tests T2 and T4 the opposite is the case. The means are not statistically significant (ANOVA, 95%, $n = 7{,}000$) over all Tests while the differences between evaporation rates of the experimental Tests (same columns) are statistically significant at 99.9% confidence interval. This shows that the difference in behavior between the two columns is not statistically significant, while the different behavior of a column between different Tests is significant. The Tukey tests confirmed that most of the pairs of evaporation rates between these Tests are not statistically different.

It should be noted that, since the evaporative conditions were changed systematically, the interpretation of these statistics should be done looking at Figure 3 and Table 1. The Tests are presented in Section 2.3 in a temporal sequence, and the changes in evaporative conditions are cumulative, so, for example, the first evaporative Test T2 is significantly different from the following evaporative Test T3. This means that the different steepness of the evaporation curves for T2 and T3 is statistically significant, that is, it is not random.

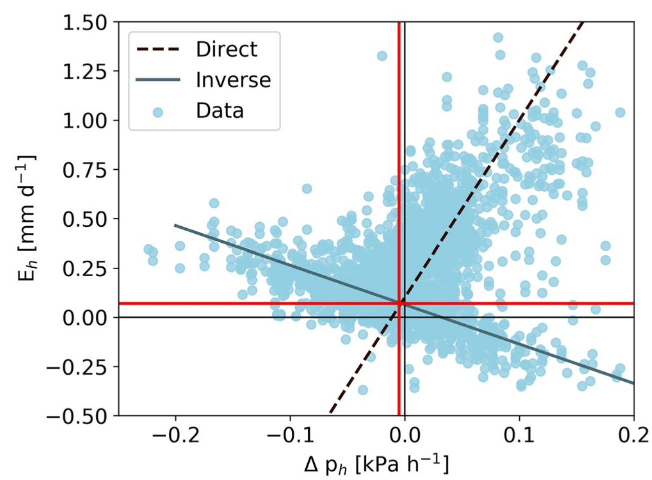

Figure 5. Scatterplot of the hourly evaporation rates (E_h) against the hourly changes in atmospheric pressure (ΔP_h), for both columns. The best fits for the positive and negative relations (described in the main text) between the data are shown. The red lines show the intersection point between the two relations. For similar graphs but presented separately per test and per short or long column, see Supplementary Materials.

3.3. Atmospheric Pressure Fluctuations Effects on Vapor Transport Through a DSL

3.3.1. Diffusion and Direct Barometric Pumping Effect

Both diffusion related evaporation estimates (Table 2), that is, one with only diffusion (Equation 1) and the other including direct barometric pumping (Equation 3), underestimated the experimental evaporation rates and neither could properly model the evaporation patterns measured in the columnar experiments. The evaporation estimated with only diffusion was 2–3 orders of magnitude smaller than the evaporation measured, and also did not follow the pattern of increases and decreases in evaporation rates between different tests. When the direct barometric pumping effect was added to the diffusion, it only marginally increased the total evaporation flux.

3.3.2. Dispersion Due to Atmospheric Pressure Fluctuations

In Figure 5, the hourly evaporation rates (E_h [mm d^{-1}]) are plotted against the corresponding hourly atmospheric pressure changes (ΔP_h [kPa h^{-1}]).

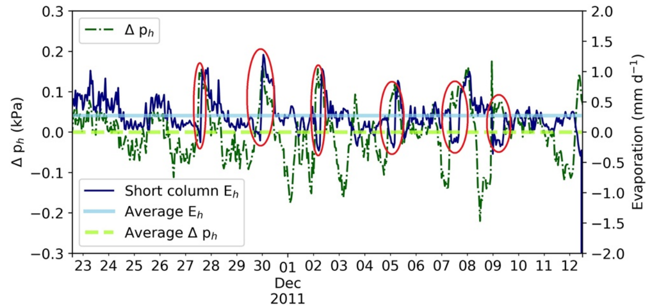

Figure 6. Hourly time series of the evaporation rates (E_h) of the short column data set T6 and atmospheric pressure changes (ΔP_h). Note that: (i) ΔP_h have zero mean (on average, the atmospheric pressure is stationary), and (ii) the average E_h is a positive quantity. The red circles show correspondence of positive ΔP_h and negative E_h.

There is a significant correlation between evaporation rates and amplitude and frequency of the atmospheric pressure fluctuations, indicating a relationship between evaporation and atmospheric pressure. We tested the hypothesis that, if the atmospheric pressure fluctuations were driving the evaporation process, then an increase in atmospheric pressure would result in an increase of the evaporation rate, and vice versa. To do so, we analyzed the correlation between the mean evaporation rate and both the mean frequency and the mean amplitude of the atmospheric pressure fluctuations in the evaporation Tests conducted, using a moving average with a window of 5 days. We found significant positive correlations between evaporation rates and both amplitude and frequency (average Pearson coefficient ~0.7) of the atmospheric pressure fluctuations: faster and with larger amplitude barometric fluctuations corresponded with larger evaporation rates.

Figure 5 shows that there are three different relations between E_h and ΔP_h: (a) a positive relation between positive ΔP_h and positive E_h; (b) a negative relation between negative values of ΔP_h (i.e., when atmospheric pressure decreases) and positive E_h, which holds for negative E_h and positive ΔP_h; (c) and a negative relation between positive ΔP_h and negative E_h. When the data set is divided in quadrants (e.g., negative E_h and negative ΔP_h, positive E_h and negative ΔP_h, etc.), it is possible to fit linear models with statistically significant correlation with $R^2 \sim 0.6$ and $p < 0.01$. Looking at Equation 4, the velocity of the gas $|V|$, dependent on ΔP_h, enters the evaporation calculation as absolute value; therefore, a mirroring effect was expected (a change from an increasing to a decreasing relationship). However, the decreasing relation in Figure 5 is also observed for positive values of ΔP_h; in our case, an increase in atmospheric pressure results in an increase of water pushed from the columns into the Mariotte bottles (a "negative evaporation" rate, $E < 0$) and vice versa. Note that the point at which the positive relation starts does not correspond to the Cartesian system origin (point 0,0 in Figure 5).

Figure 6 shows the time series of E_h and ΔP_h; the positive changes in both E_h and ΔP_h tend to have similar behavior, while the negative in the ΔP_h correspond to positive in the E_h, as expected from the absolute value sign in Equation 8. The points in which positive values of ΔP_h correspond to negative values of E_h appear always after a sudden rise of atmospheric pressure changes from negative to positive (red circles in Figure 6).

The evaporation calculated using the model presented in Equation 8 and calibrated on the short column calibration data set (T2, T3, T4), fits the evaporation rates and trends in the data sets for the short column validation data set (T6, T7, T8), as well as for the long column evaporation data set (Figures 7 and 8). The model based on Equation 8, calibrated by fitting linear models for the inverse and direct relationships for the short column T2, T3, and T4 data sets, is different from Equation 7, since we: (a) had to add a constant term inside the module function (k_3) in order to explain the shift with respect to the x axis, that was not expected by looking at Equation 7; (b) found two different multiplying coefficients (which, in the model, included both k_1 and k_3 as well), k_1^{positive} and k_1^{negative}, for the positive and negative relations between E_h and ΔP_h, respectively:

$$E_{\text{tot}} = f(\Delta P) = \begin{cases} \left| k_1^{\text{positive}} (\Delta P + k_3) \right| + k_2, \Delta P + k_3 < 0 \\ \left| k_1^{\text{negative}} (\Delta P + k_3) \right| + k_2, \Delta P + k_3 \geq 0 \end{cases} \tag{8}$$

where $k_1^{\text{positive}} = 4.91$ (mm kPa^{-1}), $k_1^{\text{negative}} = -2.00$ (mm kPa^{-1}), $k_2 = 0.07$ (mm d^{-1}), and $k_3 = 0.003$ (kPa h^{-1}). It should be noted here that the k_3 parameter fitted on the data had very low statistical significance, due to the wide spread of the data on the x axis at $E_{\text{tot}} = k_2$. A further statistical analysis could not reject the null hypothesis that $k_3 = 0$; hence, this parameter was neglected in the following analysis. The differences between Equations 8 and 7, and their applicability, are discussed in Section 4.2.

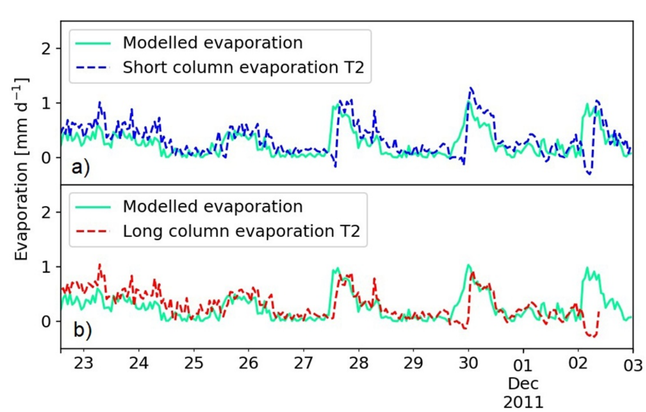

Figure 7. Hourly evaporation rates, measured and modeled using Equation 8, calibrated using short column T2, T3, and T4 evaporation data set. The evaporation is presented in the selected calibration period November 22 to December 3, 2011 (T2) for: (a) the short column (e.g., the calibration data set); (b) the long column (e.g., the verification data set).

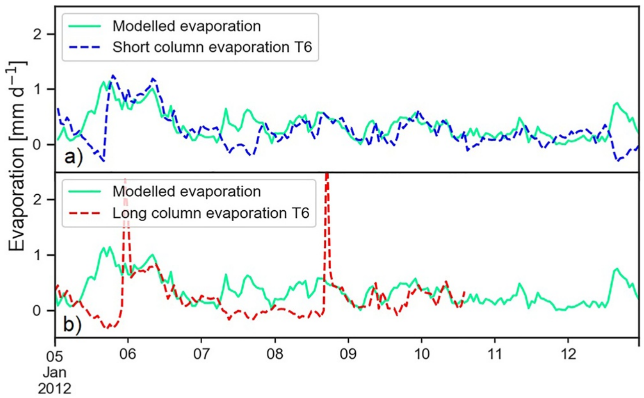

Figure 8. Hourly evaporation rates, measured and modeled using Equation 8, calibrated using short column T2, T3, and T4 evaporation data set. The evaporation is presented in the selected validation period January 5–13, 2012 for: (a) the short column; (b) the long column.

4. Discussion

4.1. Top Boundary Conditions and Experimental DSL Evaporation Rates

4.1.1. Wind Speed Effect

The effect of stable wind, with different velocities, on evaporation through a thick, >50 cm, DSL is statistically significant. The wind effect on evaporation rates can be best analyzed by comparing Tests where the wind speed was the only variable changed, that is, T2 with T3 and T7 with T8 (Table 2, Figure 4). The differences in measured evaporation rates between the Tests corresponding to different wind speeds in both columns are significant ($p < 0.05$). It should be noted that the increase in wind speed between Tests T2 and T3 is associated with a decrease in evaporation rate, in contrast to the "expected" decrease in evaporation rates between Tests T7 and T8 when wind speed decreased (Table 2, Figure 4). The unexpected decrease of evaporation between T2 and T3 can be explained by the T3 cooling effect of the wind speed at the top boundary temperature, where the wind speed changed from 0 in T2 to 1.8 m s^{-1} in T3, which resulted in a dramatic drop of the top boundary temperature from ~72°C to ~35°C, implying also substantial drop of the DSL temperature gradient. In the T7–T8 transition, instead, the change in wind speed from 1.8 to 0.3 m s^{-1} resulted in a rise in the top boundary temperature only from ~25°C to ~31°C, with a minimum effect on the DSL temperature profile, so the decrease of evaporation in both columns was likely attributed to the reduction of air turbulence.

4.1.2. Radiative Lamp Schedule (LS) Effect

The measured evaporation rates (Table 2, Figure 4) generally decreased between the Tests with 24 h continuous LS operation (T2, T3, T4) and the Tests with 12/12 on/off LS (T6, T7, T8). The paired differences of T2 and T4 with any of T6, T7 and T8 Tests were statistically significant with $p < 0.05$, in contrast to T3 pairs with any of T6, T7 and T8 (except of the T3-T8 pair for the short column that was also statistically significant); therefore, the relationship between the LS and the evaporation rates is not clear. The LS affects the top boundary temperature, with the top boundary temperature decreasing from ~32°C (T4) to ~23°C (T6), which is similar to the wind speed effect discussed in Section 4.1.1.

The temperature gradient in the DSL and, as such, the gradient of vapor densities in soil pores are a function of the top boundary temperature, which depends on both the radiative LS and the wind speed. Equation 1 supposes a correlation between the diffusion flow for water vapor in the DSL and surface temperature. If evaporation from the columns was only due to diffusion flow we would expect a direct relationship between top boundary temperature and evaporation rates. However, there is no clear relationship observed; it appears that other explanatory factors are involved in the transport of water vapor through the DSL.

The effect of changing the radiative LS from continuous to cyclic results in a reduction of evaporation rates (Figure 4; Table 2); this is in contrast to the increase that could be expected if a condensation/evaporation process was taking place. Effects of condensation and evaporation were not apparent in the columns since there was no observed change in the measured soil moisture. Therefore, the change in LS has an effect on evaporation rates but not on soil moisture in the topsoil. This could be due to the laboratory experimental conditions, where no dew forming was observed at the top of the soil column; another possible reason could be the large thickness of the DSL.

4.1.3. Z_{DSL} Thickness Effect

The relationship between Z_{DSL} and evaporation rates is not always statistically significant. The difference in evaporation rates after the first reduction of Z_{DSL} by 10 cm was statistically significant, but the difference after the second reduction of Z_{DSL} by 10 cm was not. Since the Z_{DSL} appears in the denominator in Equation 1, if all water vapor transport through the DSL was due to diffusion flow only, we would expect an inverse relationship between evaporation rates and Z_{DSL}; however even though the mean measured evaporation rates are lower in the long column than in the short column (Table 2) the difference is not statistically significant

10.1029/2020WR028286

(Section 3.2). The results do not prove that Z_{DSL} has no effect, rather, that, when Z_{DSL} is >50 cm, the effect of Z_{DSL} on evaporation rates is minimal, and that evaporation rates seem mainly dependent on some other transport process.

Many processes that increase evaporation rates for small Z_{DSL} (e.g., at least less than 5 cm, as explained in the introduction) can be negligible or even decrease evaporation rates for larger Z_{DSL} (more than 15 cm). One example is the wind effect on the evaporation rates: when the Z_{DSL} is smaller than the maximum depth of wind turbulence effect (reported to be in the orders of few centimeter), the direct effect of wind turbulence on the air distribution of a shallow profile can increase evaporation rates by actively removing water vapor from the topsoil (Davarzani et al., 2014; Mosthaf et al., 2014). However, when Z_{DSL} is larger than the maximum depth of wind turbulence effect, the only effect of wind is the change of the soil surface temperature (Section 4.1.1). Another example is the pumping out water vapor from the first centimeters of the profile caused by changes in atmospheric pressure: if $Z_{DSL} \sim 2\Delta L_{pump}$ (as defined in Equation 3, which in this study corresponds to ~2.5 and ~5 cm thick for the short and long column, respectively), the direct barometric pumping increases evaporation rates, but otherwise it has no effect on evaporation (Auer et al., 1996).

Increasing the Z_{DSL} leads to different effects, on evaporation rates, of the daily fluctuations of evaporative conditions at the top boundary, which are usually identified as the drivers of evaporation and condensation cycles in the DSL. Whenever Z_{DSL} is smaller than the depth of the maximum daily change in the soil temperature profile, the temperature change can influence the bottom of the DSL where liquid water is in equilibrium with air saturated by water vapor. In this way, the change in the temperature profile in the DSL results in an increase of evaporation because of direct transport of water vapor through condensation and evaporation cycle (Assouline et al., 2013). However, if the Z_{DSL} is larger than the damping depth of the soil temperature profile, the only effect this change has on the DSL is a decrease in average temperatures in the top boundary of the DSL (Section 4.1.2). This is what happens in this study: the maximum depth of temperature fluctuation is ~50 cm, which is comparable only with the shortest Z_{DSL} for the short column (see Table 2). The relationship between Z_{DSL} and possible evaporation processes is probably dependent on soil material properties, and should be the subject of further investigation in order to improve modeling of DSL evaporation.

4.2. Water Vapor Transport Mechanisms in the DSL

The assumption that the main water vapor transport mechanism is diffusion does not hold, even for constant evaporative conditions, and this is not related to the value of the diffusion coefficient, since the observed evaporation rate changes could not be predicted from Fick's law. This was unexpected, since previous laboratory experiments found that the diffusion flow could explain the evaporation rates measured in soil columns under stable evaporative conditions (Shokri & Salvucci, 2011; Shokri et al., 2008, 2009). This was not the case in this study (Table 2), which could be due to the much larger Z_{DSL} (>50 cm) as compared to other studies; the large distance traveled by the water vapor decreases the diffusion flow considerably, and enhances other processes that otherwise, with shorter Z_{DSL}, are less relevant (like the atmospheric pressure fluctuations effect, see below).

The process mainly responsible for the transport of water vapor through the DSL with $Z_{DSL} > 50$ cm seems to be the dispersion due to atmospheric pressure fluctuations, as indicated by the correlation between frequency and amplitude of the atmospheric pressure fluctuations and the measured evaporation rates. The direct effect of atmospheric pressure fluctuations, that is, the direct barometric pumping of air in and out of the topmost soil that reduces the thickness of the layer traveled by the water vapor (Auer et al., 1996), was shown to be of less relevance in this study (Table 2) as it is at least one order of magnitude smaller than the measured evaporation rates.

Equation 8 derived in this study allowed to model the behavior of the measured evaporation time series in both the validation data set for the short column (T6, T7, and T8) and the evaporation measured in the long column (verification data set), as shown in Figures 7 and 8. Given these results, the model appears to be robust, at least for the soil properties and Z_{DSL} studied. The effect of atmospheric pressure fluctuations on the evaporation rates is shown in Figure 3 (all the other boundary conditions are kept constant). Another possible sources of the fluctuations in evaporation rates reported in Figure 3 could be the heterogeneity in the soil column material packing, or random errors. As the fluctuations appear to have the same behavior in short and long columns, the effect of soil heterogeneity and of the randomness can be ruled out, pointing at the impact of atmospheric pressure fluctuations.

One reported effect of atmospheric pressure fluctuations on groundwater is that they directly affect the water pressure in the column, resulting in fluctuations in the water levels. This effect probably plays a role in the negative relation between E_h and ΔP_h shown in Figure 6. However, the hypothesis that the effect of atmospheric pressure fluctuations was limited to fluctuations in the water level in the columns can be ruled out, since this would result in fluctuations without long-term trend due to evaporation. When considering the long-term average of the evaporation rates the pressure fluctuations cancel out, and only the long time trend evaporation would be recorded (see the average E_h in Figure 6). Moreover, this hypothesis is disproved by the fact that the measured Mariotte bottle's weight changes were larger than those predicted using the equation for water table fluctuations by Rojstaczer and Riley (1990). In field conditions, such static fluctuations would have an effect on evaporation rates only for shallow water table depths, due to the changes in Z_{DSL}.

The results of the model represented by Equation 8 and based on Equations 4 and 6, indicate that E_h is dependent on ΔP_h (Table 2 and Figure 8). The minor differences between the physical equation as Equation 7 and the model using Equation 8, however, need to be explained. The main difference is that, in Equation 8, there are two empirical coefficients (one for the negative and one for the positive relation) instead of only one. Note, the empirical coefficients k_1^{positive} and k_1^{negative} represent the efficiency with which the barometric fluctuation extracts the water vapor from the column (a combination of α and other soil material properties), and they switch from one to the other when either the air above the column is pushed inside the column, or the air in the column is pulled out of the column. Such gas transport in soils, with compression and expansion behavior, was observed for CO_2 flow in similar, semi-arid conditions of sandy soil, dry topsoil (see Figure 6 in Sánchez-Cañete et al., 2013).

It is possible to explain the need for two different coefficients (k_1^{positive} and k_1^{negative}) for the dependence of E_h on ΔP_h by looking at Equation 6, where the terms $\frac{dC}{dz}\alpha\frac{1}{P_0}\left(L - z\right)\omega\sin\left(\omega t\right)$ are simplified into the empirical parameter k_1. This simplification is based on the assumption that all the terms simplified are independent of the sign of ΔP_h, that is, they do not change their values between a compression or an expansion cycle. However, this may not hold true for the term $\frac{dC}{dz}$: during a compression cycle ($\Delta P_h > 0$), air from above the soil is pumped inside the soil column, and hence the vapor concentration gradient between the saturation value at vaporization plane and atmospheric value at soil surface gets compressed within a distance $2\Delta L_{\text{pump}}$. In the same way, during an expansion cycle ($\Delta P_h < 0$) the air inside the soil column is pumped out into the atmosphere, and the gradient is extended equally within a distance $2\Delta L_{\text{pump}}$. Therefore, it is expected that $\frac{dC}{dz}$ has a larger value when $\Delta P_h > 0$ and a smaller value when $\Delta P_h < 0$, that is exactly what happens to k_1 in this case.

5. Conclusions

We found that the main process of water vapor transport through a thick DSL is not diffusion but atmospheric pressure fluctuations, actually composed of two different processes, dispersion and direct barometric pumping, both dependent on atmospheric pressure fluctuations. The first process happens when air saturated with water vapor is pulled out of the column while atmospheric pressure decreases. The second process happens when the atmospheric pressure increases and air is pushed inside the soil, displacing the water vapor saturated air from the soil. More in detail, we found that:

- The assumption of only diffusion flow with thick Z_{DSL} does not hold, even for the experiment with constant evaporative conditions.
- The wind effect and daily radiation cycles had only very small effect on the evaporation rates with a $Z_{\mathrm{DSL}} > 50$ cm.

- The diffusion flow, mechanical dispersion flow, and direct barometric pumping effects, could not explain fluctuations of evaporation rates measured in the experiments (Figure 3).
- The model based on Equation 8 was able to simulate the measured evaporation rates, their trends and their fluctuations (Figures 7 and 8).
- The evaporation measured was found to be mainly dependent on atmospheric pressure fluctuations effect on the water vapor in the DSL, with two processes driving water vapor flow mechanism: direct barometric pumping and dispersion.

The findings of the study indicate that the relevant processes of water vapor transport in the thick DSL are different from the processes in the thin DSL, with thick and thin defined by the depth at which these transport processes change their magnitude. The evaporation rates found in this study with the thick DSL are relevant because: (a) DSL with comparable thickness have been typically reported in field conditions in semi-arid and arid areas; (b) the measured water vapor transport is the basis to understand how Z_{DSL} influences evaporation rates in presence of a DSL (Balugani et al., 2017; McColl et al., 2017); (c) the evaporation rates measured in this study, that is, in the presence of the thick DSL, confirmed that assuming soil evaporation as occurring mainly due to diffusion flow substantially underestimates the evaporation.

Further studies should try to: (a) define how the relevant processes of water vapor transport through a DSL (atmospheric fluctuations, diffusion, daily cycles of evaporation/condensation, wind) change with increasing Z_{DSL}, testing different evaporative conditions on soil columns with different imposed Z_{DSL}; (b) validate the Equation 8, especially its k-coefficients, which need to be checked with other soil materials and with wider range of ZDSL; (c) test the results of this laboratory study under field conditions.

Data Availability Statement

The whole data set is available at https://data.mendeley.com/datasets/s63crvbgh2/1.

Acknowledgments
This research was supported by the International Institute for Geo-Information Science and Earth Observation (ITC), Faculty of University of Twente (the Netherlands). The authors thank the five anonymous reviewers and the Water Resources Research editorial team (Editor D. Scott Mackay and an anonymous Associate Editor) for the constructive and helpful comments.

References

Assouline, S., Tyler, S. W., Selker, J. S., Lunati, I., Higgins, C. W., & Parlange, M. B. (2013). Evaporation from a shallow water table: Diurnal dynamics of water and heat at the surface of drying sand. *Water Resources Research*, *49*(7), 4022–4034. https://doi.org/10.1002/wrcr.20293

Auer, L. H., Rosenberg, N. D., Birdsell, K. H., & Whitney, E. M. (1996). The effects of barometric pumping on contaminant transport. *Journal of Contaminant Hydrology*, *24*(2), 145–166. https://doi.org/10.1016/S0169-7722(96)00010-1

Balugani, E., Lubczynski, M. W., Reyes-Acosta, L., van der Tol, C., & Francés, A. P. (2017). Groundwater and unsaturated zone evaporation and transpiration in a semi-arid open woodland. *Journal of Hydrology*, *547*, 54–66.

Balugani, E., Lubczynski, M. W., van der Tol, C., & Metselaar, K. (2018). Testing three approaches to estimate soil evaporation through a dry soil layer in a semi-arid area. *Journal of Hydrology*, *567*, 405–419. https://doi.org/10.1016/j.jhydrol.2018.10.018

Bear, J. (1972). *Dynamics of fluids in porous media*. American Elsevier.

Bestelmeyer, B. T., Okin, G. S., Duniway, M. C., Archer, S. R., Sayre, N. F., Williamson, J. C., & Herrick, J. E. (2015). Desertification, land use, and the transformation of global drylands. *Frontiers in Ecology and the Environment*, *13*(1), 28–36. https://doi.org/10.1890/140162

Brutsaert, W. (2014). Daily evaporation from drying soil: Universal parameterization with similarity. *Water Resources Research*, *50*, 3206–3215. https://doi.org/10.1002/2013WR014872.Received

Davarzani, H., Smits, K., Tolene, R. M., & Illangasekare, T. (2014). Study of the effect of wind speed on evaporation from soil through integrated modeling of the atmospheric boundary layer and shallow subsurface. *Water Resources Research*, *50*(1), 661–680. https://doi.org/10.1002/2013WR013952

Deol, P. K., Heitman, J. L., Amoozegar, A., Ren, T., & Horton, R. (2014). Inception and Magnitude of Subsurface Evaporation for a Bare Soil with Natural Surface Boundary Conditions. *Soil Science Society of America Journal*, *78*(5), 1544. https://doi.org/10.2136/sssaj2013.12.0520

Dijkema, J., Koonce, J. E., Shillito, R. M., Ghezzehei, T. A., Berli, M., Ploeg, M. J., et al. (2017). Water distribution in an arid zone soil: Numerical analysis of data from a large weighing lysimeter. *Vadose Zone Journal*, *17*, 170035. https://doi.org/10.2136/vzj2017.01.0035

Grifoll, J. (2013). Contribution of mechanical dispersion of vapor to soil evaporation. *Water Resources Research*, *49*(2), 1099–1106. https://doi.org/10.1002/wrcr.20105

Idso, S. B., Reginato, R. J., & Jackson, R. D. (1979). Calculation of evaporation during the three stages of soil drying. *Water Resources Research*, *15*(2), 487–488. https://doi.org/10.1029/wr015i002p00487

Koonce, J. (2016). *Water balance and moisture dynamics of an arid and semi-arid soil: A weighing lysimeter and field study* (UNLV Theses, Dissertations, Professional Papers, and Capstones). Retrieved from http://digitalscholarship.unlv.edu/thesesdissertations/2692

Kuang, X., Jiao, J. J., & Li, H. (2013). Review on airflow in unsaturated zones induced by natural forcings. *Water Resources Research*, *49*(10), 6137–6165. https://doi.org/10.1002/wrcr.20416

Lampinen, M., Assad, M. El H., & Curd, E. F. (2001). Physical fundamentals. In H. Goodfellow & E. Tähti (Eds.), Industrial ventilation design guidebook (pp. 41–171). https://doi.org/10.1016/B978-012289676-7/50007-2

Lehmann, P., Assouline, S., & Or, D. (2008). Characteristic lengths affecting evaporative drying of porous media. *Physical Review E*, *77*(5).

Massman, W. J. (2006). Advective transport of CO_2 in permeable media induced by atmospheric pressure fluctuations: 1. An analytical model. *Journal of Geophysical Research*, *111*(3). https://doi.org/10.1029/2006JG000163

McColl, K. A., Wang, W., Peng, B., Akbar, R., Lu, H., Pan, M., et al. (2017). Global characterization of surface soil moisture drydowns. *Geophysical Research Letters*, *44*, 1–9. https://doi.org/10.1002/2017GL072819

Moldrup, P., Olesen, T., Gamst, J., Schjønning, P., Yamaguchi, T., & Rolston, D. E. (2000). Predicting the gas diffusion coefficient in repacked soil. *Soil Science Society of America Journal*, *64*(5), 1588. https://doi.org/10.2136/sssaj2000.6451588x

Mosthaf, K., Helmig, R., & Or, D. (2014). Modeling and analysis of evaporation processes from porous media on the REV scale. *Water Resources Research*, *50*, 1059–1079. https://doi.org/10.1002/2016WR018954.Received

Neriah, A. B., Assouline, S., Shavit, U., & Weisbrod, N. (2014). Impact of ambient conditions on evaporation fromporous media. *Water Resources Research*, *50*, 6696–6712. https://doi.org/10.1002/2014WR015523.Received

Or, D., Lehmann, P., Shahraeeni, E., & Shokri, N. (2013). Advances in soil evaporation physics—A review. *Vadose Zone Journal*, *12*(4). https://doi.org/10.2136/vzj2012.0163

Parsons, A. J., & Abrahams, A. D. (1994). Geomorphology of desert environments BT. In A. D. Abrahams, & A. J. Parsons (Eds.), Geomorphology of desert environments (pp. 3–12). Springer Netherlands. https://doi.org/10.1007/978-94-015-8254-4_1

Rojstaczer, S., & Riley, F. S. (1990). Response of the water level in a well to Earth tides and atmospheric loading under unconfined conditions. *Water Resources Research*, *26*(8), 1803–1817. https://doi.org/10.1029/WR026i008p01803

Sánchez-Cañete, E. P., Kowalski, A. S., Serrano-Ortiz, P., Pérez-Priego, O., & Domingo, F. (2013). Deep CO_2 soil inhalation/exhalation induced by synoptic pressure changes and atmospheric tides in a carbonated semiarid steppe. *Biogeosciences*, *10*(10), 6591–6600. https://doi.org/10.5194/bg-10-6591-2013

Shokri, N., Lehmann, P., & Or, D. (2009). Critical evaluation of enhancement factors for vapor transport through unsaturated porous media. *Water Resources Research*, *45*(10). https://doi.org/10.1029/2009WR007769

Shokri, N., Lehmann, P., Vontobel, P., & Or, D. (2008). Drying front and water content dynamics during evaporation from sand delineated by neutron radiography. *Water Resources Research*, *44*(6). https://doi.org/10.1029/2007WR006385

Shokri, N., & Or, D. (2011). What determines drying rates at the onset of diffusion controlled stage-2 evaporation from porous media? *Water Resources Research*, *47*. https://doi.org/10.1029/2010WR010284

Shokri, N., & Salvucci, G. D. (2011). Evaporation from porous media in the presence of a water table. *Vadose Zone Journal*, *10*, 1309–1318.

Sun, P., Ma, J., Qi, S., Zhao, W., & Zhu, G. (2016). The effects of a dry sand layer on groundwater recharge in extremely arid areas : Field study in the western Hexi Corridor of northwestern China. *Hydrogeology Journal*, *24*, 1515–1529. https://doi.org/10.1007/s10040-016-1410-2

Vanderborght, J., & Vereecken, H. (2007). Review of dispersivities for transport modeling in soils. *Vadose Zone Journal*, *6*(1), 29. https://doi.org/10.2136/vzj2006.0096

Wang, X. (2015). Vapor flow resistance of dry soil layer to soil water evaporation in arid environment: An overview. *Water*, *7*(8), 4552–4574. https://doi.org/10.3390/w7084552

Zeng, Y., Wan, L., Su, Z. B., Saito, H., Huang, K. L., & Wang, X. S. (2009). Diurnal soil water dynamics in the shallow vadose zone (field site of China University of Geosciences, China). *Environmental Geology*, *58*(1), 11–23.